

Energy-efficient building spatial layout strategies under future climate change scenarios

Pengyuan Shen^{1,*}, Yanxiang Yang¹, Lingyao Li¹, Jie Zhong¹

¹ Institute of Future Human Habitat, Shenzhen International Graduate School, Tsinghua University, Shenzhen 518055, China

*Corresponding Author: Pengyuan_pub@163.com

Abstract

This study explores the impact of future climate change on energy-efficient building spatial layout and identifies adaptation strategies under different climate scenarios. Existing research mainly focuses on optimizing spatial layouts for current climate conditions, overlooking long-term energy performance. To address this gap, this study employs an energy-efficiency-oriented spatial layout optimization method and a distribution-adjusted temporal mapping (DATM) technique for future climate prediction. A standard office building model is analyzed under the current climate condition and five SSP scenarios (2030–2059). Results show that future climate change significantly affects spatial layout energy performance, with operational energy consumption increasing by at least 25.84% under SSP126 (energy-efficient building spatial layout under current climate condition). Layouts optimized for current conditions decline in efficiency under future climates, emphasizing the need for adaptive design. Clustering and statistical analyses reveal that orientation, division, and adjacency relationships are key to energy efficiency across climate scenarios. Findings suggest that flexible zoning, reconfigurable layouts, and dynamic adjacency strategies are essential for climate-adaptive design. By providing quantitative insights and design recommendations, this study establishes a methodological foundation for integrating future climate considerations into pre-design phase building design.

Key words : Spatial layout, Climate change, Energy efficiency, Climate-adaptive design, Optimization

Key Innovations

The study introduces a novel methodology combining energy-efficiency-oriented spatial layout optimization with distribution-adjusted temporal mapping for future climate prediction. Through comprehensive analysis of building spatial layouts across multiple climate scenarios, it reveals that current energy-efficient layouts significantly decline in performance under future climate conditions, identifying critical adaptation thresholds.

Practical Implications

Building designers must prepare for at least 25% higher energy consumption in currently optimized buildings

under future climate scenarios. The study provides actionable spatial design strategies including orientation along east-west axes, moderately complex zoning (ZC_3), and strengthened adjacency relationships (Nei_3-4) to enhance climate resilience, with specific recommendations for short, medium, and long-term adaptation.

Introduction

Reducing building operational energy, which accounts for over 30% of global consumption, is crucial in the context of global warming (IEA, 2019). Due to its preemptive nature and difficulty in modification, the pre-design phase has a particularly significant impact on operational energy consumption. According to one study, over 40% of energy-saving potential originates from the pre-design phase (Hemsath, 2013). Therefore, investigating building energy performance during pre-design is essential for reducing carbon emissions and achieving carbon neutrality goals.

Current research on energy-efficient design primarily focuses on building form and façade performance, with limited attention to the relationship between spatial layout and energy performance (Shen, Li, Gao, Chen, et al., 2025). While studies have shown that spatial layout impacts energy consumption under fixed building envelopes (Cheng et al., 2016; Du et al., 2020, 2021; Latha et al., 2023; Musau & Steemers, 2008), their applicability to multi-story buildings with complex functions remains limited, and automation in layout optimization is underdeveloped. Additionally, most energy-efficient design research relies on current climate data, failing to account for long-term climate changes that significantly affect building energy performance.

Currently, research in this field has demonstrated that a defined energy-efficient spatial layout strategies exists under a specific climate scenario (Du, 2021). However, the future adaptability of such strategies has not been effectively validated. Accordingly, this study aims to address the following three key questions.

1. Will the energy-efficient spatial layout under current climate scenario still be efficient in the future?

2. What is the relationship between the energy-efficient spatial layout and different future climate scenarios?
3. What are the design strategies for energy-efficient spatial layout in response to future climate change?

To address these questions, this study explores energy-efficient spatial layouts under future climate scenarios, examining their relationship with different climate scenarios. Using an optimization framework combined with a distribution-adjusted temporal mapping (DATM) method for climate prediction, this research provides a methodological foundation for integrating climate resilience into building pre-design.

Methodology

Energy-Efficiency Oriented Spatial Layout Generation and Optimization Method

This method, based on a reverse workflow in automated building design, addresses the energy-efficient functional spatial layout in high-rise office buildings. It consists of two main components: a 3D functional spatial layout algorithm module (GSL) implemented through a custom Python algorithm and an energy performance optimization module (EPO) using the Octopus tool. By following predefined rules and parameters, this method can generate diverse building layout solutions and iteratively optimize them with an energy-efficiency objective.

Automatic Generation of Space Layouts(GSL) Method

GSL module first establishes a grid model by drawing on fundamental principles from digital image processing(Jähne, 2005), segmenting the building model into a three-dimensional spatial grid and assigning different functional attributes to each unit. Layout generation is then conducted using a custom algorithm (Figure 1). The GSL module generates 3D spatial layouts by applying state transition rules to adjacent spatial units (Figure 2).

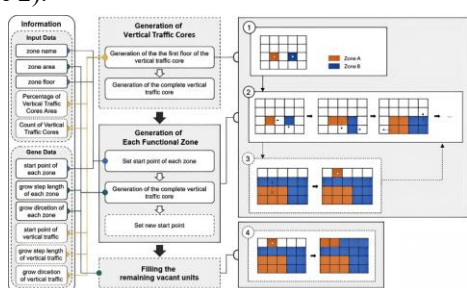


Figure 1: 3D space generation algorithm

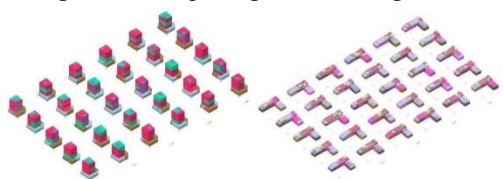


Figure 2: Algorithm layout generation schematic

Energy Performance Optimization(EPO) Method

EPO module utilizes the Octopus plugin(Manni, Lobaccaro, Lolli, & Bohne, 2020; Toutou, Fikry, & Mohamed, 2018), which is based on a genetic algorithm, as the iterative optimization tool. Energy simulation is conducted using the Honeybee plugin(Tabadkani, Shouibi, Soflaei, & Banihashemi, 2019), which integrates EnergyPlus as the core engine. This module enables energy-driven iterative optimization of 3D spatial layout solutions.

To evaluate the energy performance of spatial layout solutions, building annual energy load per unit area is used as the key objective. The annual energy load per unit area (Annual_Load), measured in kWh/m², represents the total energy consumption of a building over a year divided by its total floor area. This includes energy consumption for heating, cooling, lighting, and equipment operation (1).

$$E_{annualLoad} = Q_{heating} + Q_{cooling} + Q_{lighting} + Q_{equipment} \quad (1)$$

Workflow of GSL-EPO

Within GSL-EPO framework (Figure 3), the EPO module first provides genetic parameters, which the GSL module then uses to generate a spatial layout solution. Subsequently, the EPO module evaluates the energy performance of this solution through simulation and iteratively optimizes it by generating new genetic parameters.

Through this iterative optimization workflow, increasingly energy-efficient spatial layout solutions are continuously generated. Additionally, by analyzing the iteration process and convergence trends, the method can approximate the optimal energy performance solution as closely as possible.

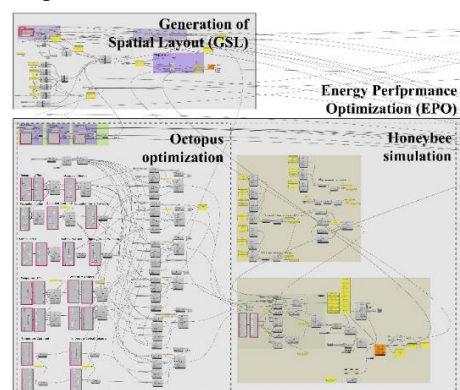


Figure 3: Workflow of GSL-EPO framework

Future Hourly Weather Data Downscaling Method

Building Performance Simulation (BPS) is a critical tool for predicting a building's thermal behavior, energy consumption, and indoor comfort under future climate scenarios (Wang & Zhai, 2016). Accurate BPS relies on precisely predicted future climate data. However, the spatial resolution of Global Climate Model (GCM) outputs is too coarse to capture localized climate variations and specific weather patterns that affect individual buildings(Laflamme, Linder, & Pan, 2016).

Therefore, GCM outputs must be downscaled into high-resolution local climate data to guide architects in designing resilient and energy-efficient buildings for future climates (Andrić, Koc, & Al-Ghamdi, 2019; Shen, 2024; Shen, Li, Gao, Zheng, et al., 2025).

Distribution Adjusted Temporal Mapping(DATM) Method

In this method, future climate data prediction is based on a self-made Distribution Adjusted Temporal Mapping (DATM) method. This method downscale monthly Global Climate Model (GCM) data into hourly future climate data, using Typical Meteorological Year (TMY) data as the baseline (Shen, 2025). The proposed method involves three key steps: (1)Fitting probability distributions to each climate variable in the TMY dataset. (2)Modifying these distributions based on the monthly changes predicted by GCM. (3)Mapping future hourly weather data from the adjusted distributions.

Advantages of DATM method in the field of Building Performance Simulation(BPS)

In the field of BPS, existing statistical downscaling methods such as the Super Resolution Deep Residual Network(Laflamme et al., 2016) and weather generators (Laflamme et al., 2016) have shown promising accuracy but often require specific long-term datasets and computational resources that exceed the typical capacity of BPS workflows. As a result, approximately 33% of studies in this domain continue to rely on the morphing method due to its simplicity and compatibility with widely available TMY data.

Compared to these methods, the proposed DATM method achieves a balance between high accuracy and implementation feasibility (Shen, 2025). Through comparison with the morphing method, DATM demonstrates superior performance in capturing temperature extremes, accurately modeling the tails of relative humidity distributions, and maintaining the physical constraints of solar radiation. Validation using onsite hourly weather data from 2015 to 2024 confirms that DATM offers higher statistical consistency and distributional fidelity across most climate variables (Shen, 2025). Figure 4 illustrates the improved reliability of the DATM method over the morphing method in predicting extreme climate events.

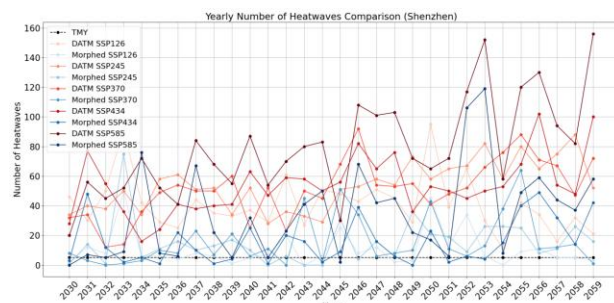


Figure 4: Yearly number of heatwaves comparison in Shenzhen

Materials

Future Climate Scenarios

The future climate scenario data used in this study were obtained through the DATM method described above. The Global Climate Model (GCM) employed is MRI-ESM2-0, developed by the Meteorological Research Institute of Japan (Shen, Ji, et al., 2025; Yukimoto et al., 2019). Additionally, the study utilizes GCM outputs based on the latest Shared Socioeconomic Pathways (SSPs) (O'Neill et al., 2014).

SSPs are a collection of five narrative-based, globally applicable, and coherent storylines of possible future developments in greenhouse gas emissions, land use, and economic growth, among other factors(Riahi et al., 2017). The SSPs considered in this study include:

- SSP1-2.6: Low emissions, strong climate action, warming kept below 2°C.
- SSP2-4.5: Moderate emissions, current development trends with some mitigation.
- SSP3-7.0: High emissions, limited development, ineffective climate policies.
- SSP4-3.4: Moderate emissions, some mitigation and adaptation measures.
- SSP5-8.5: Very high emissions, fossil fuel reliance, severe climate impact.

Hereafter, the five future climate scenarios are abbreviated as SSP126, SSP434, SSP245, SSP370, and SSP585, while the current climate condition is abbreviated as TMY.

Experiment Model: Standard Office Building Model

A standard office building model is selected as the experimental subject. The model is based on the Commercial Reference Buildings developed by the U.S. Department of Energy. The office building consists of eight floors, each with a floor height of 3.6 m, a footprint of 1,536 m², and a total area of 12,288 m² (Figure 5). The standard floor has a length-to-width ratio of 3:2, with the building oriented due south and the site located in Shenzhen, Guangdong, China.

Following the method described before, the building is divided into 24 grid units per floor, totaling 192 grid units across eight floors. The floor plan and grid division are shown in Figure 5. The central area is designated for vertical circulation and auxiliary functions, and is therefore excluded from the functional layout arrangement.

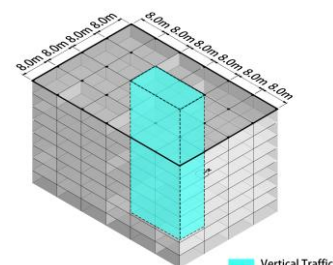


Figure 5: Standard office building model

Experiment Parameters

The office building is divided into five functional zones and one circulation zone. The area proportions and

parameter details for each zone are summarized in Table 1. For ease of expression, the abbreviations for each functional zone hereafter are listed.

Table 1: Energy consumption simulation parameters for each functional zone

Function Name	Area (m ²)	Area (m ² /person)	Electrical equipment power density (W/ m ²)	Lighting power density (W/ m ²)
Open Office(Zone 1)	4608	10	15	8
Closed Office(Zone 2)	2560	15	15	8
Serviced Apartment(Zone 3)	1536	25	15	6
Sessions(Zone 4)	1280	10	12	12
Cafeteria(Zone 5)	1280	8	13	12
Vertical Traffic	1024	8	5	6

The experiment assumes traditional lighting design, making lighting and equipment loads dependent only on building area. Envelope materials are listed in Table 2. The window-to-wall ratio is 40% for north and south façades and 20% for east and west, modeled using Honeybee's "HB Apertures by Ratio" module. Shenzhen's heating and cooling periods follow relevant standards (Table 3), while occupancy, equipment, lighting, and HVAC schedules adhere to common parameters.

Table 2: Material parameters of the envelope

Building envelope	Material	K (W/m ² ·K)
External wall	Pure gypsum board 10mm + Extruded polystyrene board 60mm + Pure gypsum board 8mm + Heavy mortar clay 240mm	0.45
Roof	Bituminous mineral wool 25mm + extruded polystyrene board 50mm + bituminous mineral wool felt 30mm	0.53
Interior wall	Cement mortar 20mm + ceramic concrete 180mm + cement mortar 20mm	3.57
Windows	6 High Transmittance Low-E+12 Air+6 Transparent Thermal insulated metal profiles	2.70

Table 3: Heating/Cooling period of Shenzhen)

City	The cooling period	The heating period
Shenzhen	6.1 -9.31	11.15 -3.15

In this experiment, the areas of each functional zone, building envelope materials, window-to-wall ratios, and other key parameters are kept constant. Only the spatial layout of the functional zones is adjusted and changed to rigorously evaluate the impact of spatial layout — considered as an independent variable — on building

energy performance. Therefore, only the Annual_Load is selected as the single-objective optimization metric, and the feasibility of the generated spatial layout solutions is not overly considered at this stage.

The experiment includes six climate scenarios: Shenzhen's current climate (TMY) and five future scenarios (SSP126, SSP434, SSP245, SSP370, SSP585). Each scenario generates 1,800 optimized solutions through 30 generations of 60 solutions each (Figure 6). Hyper-parameters of the genetic algorithm are adjusted, and the final dataset is selected when the Annual_Load difference among the top three solutions is under 1%, minimizing local optima risk.

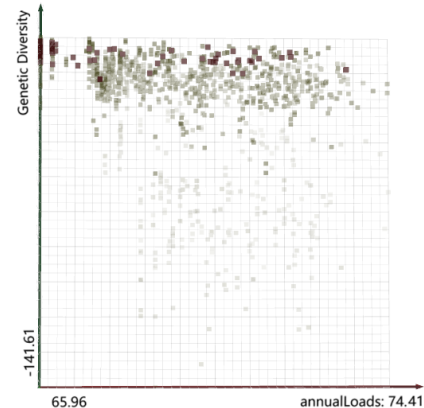


Figure 6: GSL-EPO experiment

Post-optimization Analysis

The six spatial layout solution sets are processed by removing duplicates from optimization convergence. Each climate scenario retains 800–900 valid solutions.

For the spatial layout solution sets, their 3D models (Figure 7) are difficult to observe and directly compare to derive convincing data-driven conclusions. Therefore, spatial layout features are needed to quantify the architectural properties of spatial layouts into numerically measurable data indicators.

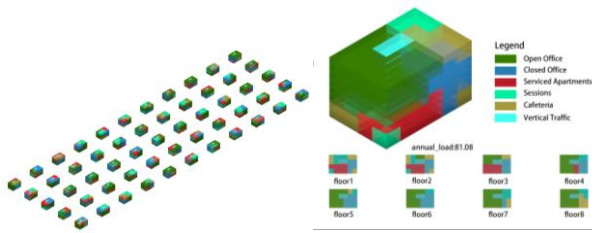


Figure 7: Spatial layout solution set

Spatial Layouts Features Extraction

The properties of spatial layouts include layout dimensions, interior partitions, and the locations of different functions. In this study, we focus the analysis of spatial layout features on three key aspects: the orientation of different function zones, the segmentation of different function zones, and the adjacency between different function zones. These aspects are quantified into the following three types of data indicators:

- **Orientation Feature** represents the distribution of a functional zone in a specific direction. For example, Ori_1N indicates the distribution of Function Zone 1 in the north direction. Its value is calculated as the proportion of Function Zone 1's grid that are adjacent to the northern boundary. A higher value means that the function is more concentrated toward that orientation.
- **Division Feature** represents the segmentation of a functional zone. For example, ZC_1 represents the number of separate, non-adjacent parts into which Function Zone 1 is divided. A higher value indicates that the function is more fragmented.
- **Neighbor Feature** represents the adjacency between different functional zones. For example, Nei_1-2 indicates the adjacency between Function Zone 1 and Function Zone 2. Its value is calculated as the total length of adjacent grid edges between these two zones. A higher value suggests that the two functional areas are more closely positioned.

Analysis Method

This section explains the analysis methods for the solution data sets. Due to the complexity and high dimensionality of the data related to different functional zones and their corresponding three types of spatial layout features, it is difficult to form a concise representation of the spatial layout feature for a given solution. Therefore, the data analysis method follows the following three steps.

(1) Principal Component Analysis (PCA) is applied to condense the three spatial layout feature types into a lower-dimensional representation, facilitating comparison between solutions. (2) To account for randomness in individual solutions, K-means clustering groups solutions into high- and low-energy-consumption clusters based on Annual_Load, with the optimal cluster count determined by the elbow method. (3) Analysis of Variance (ANOVA) for Heterogeneity Analysis: ANOVA ($p < 0.01$) assesses variations in spatial layout features across clusters, identifying statistically significant differences. These steps collectively reveal spatial layout distinctions under different climate scenarios.

Results

Energy Use in Future Climate Scenarios

From the K-means clustering analysis under a single climate scenario (Figure 8) (taking SSP370 as an example), it can be observed that different Annual_load clusters exhibit a clear stratification in PCA component—which represents spatial layout features. This also confirms the existing research conclusion that a defined energy-efficient spatial layout strategy exists under a specific climate scenario.

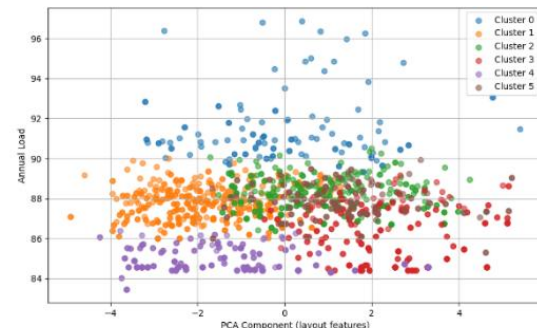


Figure 8: Solutions clustering (SSP370)

Analyzing the relationship between energy-efficient spatial layout and different climate scenarios, it is evident from the Annual_Load values of the energy-efficient spatial layouts under various climate scenarios that climate change has a significant impact on building operational energy consumption (Table 4). The energy-efficient spatial layout under TMY will experience a substantial increase in operational energy consumption under future climate conditions. Even under the mildest SSP126, the annual_load will rise by 25.84%.

Table 4: Energy-efficient spatial layout (EESL) Annual_load rise

Annual_load(kWh/m ²)	TMY	SSP126	SSP 245	SSP 370	SSP 434	SSP 585
EESL of TMY	72.96	91.81	89.64	90.26	89.39	93.38
EESL	/	84.14	82.35	83.45	81.08	85.43

Also taking SSP126 as an example, the Annual_Load of the energy-efficient spatial layout under TMY is 91.81 kWh/m², while under SSP126, it is 84.14 kWh/m². This difference initially reveals that energy-efficient spatial layout varies significantly across future climate scenarios. To verify whether there is a consistent difference, ANOVA check of the lowest Annual_Load clusters across climate scenarios results show significant heterogeneity in most indicators.

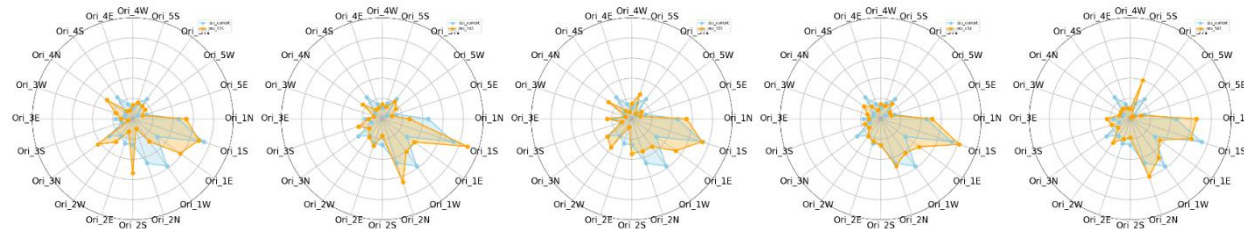


Figure 9: Comparison of TMY and SSP126/ SSP245/ SSP370/ SSP434/ SSP585 in orientation feature

For Orientation Features, under the current climate condition(TMY), the orientation distribution remains relatively balanced, predominantly aligned along the northeast-southwest (ORI_NE to ORI_SW) axis. This distribution likely results from the need to balance solar gain and thermal control under present climatic conditions. In the low-emission scenario (SSP126), the optimized orientation begins to shift towards the east-west axis (ORI_E and ORI_W) while still maintaining some degree of dispersion. This pattern suggests that only minor adjustments to the orientation strategy are necessary under mild climate change conditions. For moderate-emission scenarios (SSP245 and SSP370), the optimized orientation becomes significantly concentrated along both the northeast-southwest and east-west axes, exhibiting a stronger directional preference. This shift is likely a

Relationship between Spatial Layout and Future Climate Scenarios

To further analyzes this heterogeneity, we compared the lowest Annual_Load clusters' spatial layout features between different SSP scenarios and TMY scenarios, as well as among different SSP scenarios, the following patterns can be summarized.

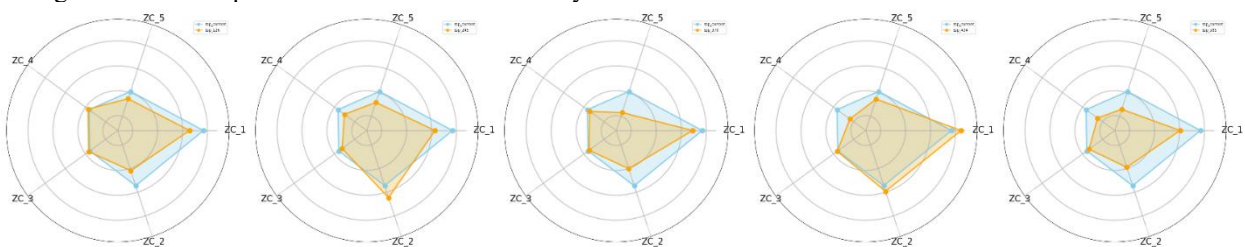


Figure 10: Comparison of TMY and SSP126/ SSP245/ SSP370/ SSP434/ SSP585 in division feature

For Division Features, under the current climate condition(TMY), the zoning distribution is relatively balanced, ranging between ZC_2 and ZC_4, reflecting the diverse spatial requirements under existing climatic conditions. In the low-emission scenario (SSP126), zoning begins to concentrate around ZC_3, indicating that integrating certain functional areas is more advantageous for energy optimization under mild climate changes. For moderate-emission scenarios (SSP245 and SSP370), the proportion of ZC_3 and ZC_4 increases, while ZC_1 and ZC_2 decrease. This trend suggests that as climate warming intensifies, more refined zoning strategies are required to effectively manage varying thermal loads.

response to increasing cooling demands associated with rising temperatures. In the high-emission scenario (SSP585), the orientation is almost entirely concentrated along the east-west axis (ORI_E), with a near-complete abandonment of the north-south orientation. This trend may be attributed to the need to minimize summer overheating risks while simultaneously maximizing passive solar gain during winter months.

Across all future climate scenarios, a clear trend emerges: as emission levels increase, the optimal orientation becomes progressively more concentrated, with a narrowing distribution range. This suggests that under intensified climate warming, the flexibility in architectural orientation selection decreases, necessitating more precise and deliberate design strategies.

In the high-emission scenario (SSP585), zoning becomes highly concentrated in ZC_3, with ZC_1 nearly disappearing. This pattern implies that under extreme climate warming, a moderately complex zoning strategy is the most effective for energy management.

Across all future climate scenarios, zoning transitions from a dispersed distribution under TMY to a more concentrated configuration under SSP585. However, this shift does not follow a strictly linear progression but rather exhibits a “first dispersed, then concentrated” pattern. This suggests that a medium level of zoning complexity provides the greatest adaptability to future climate conditions.

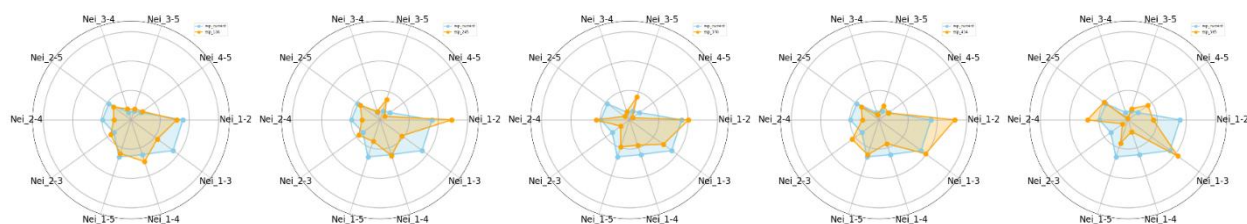


Figure 11: Comparison of TMY and SSP126/ SSP245/ SSP370/ SSP434/ SSP585 in neighbor feature

For Neighbor Features, under the current climate condition(TMY), adjacency relationships are relatively balanced, with Nei_1-2, Nei_2-3, and Nei_3-4 exhibiting similar distributions. This reflects the diverse spatial connectivity needs under existing climate conditions. In the low-emission scenario (SSP126), adjacency relationships begin to shift towards Nei_2-3 and Nei_3-4, suggesting an increased emphasis on heat buffering and transfer efficiency between functional zones under mild climate changes. For moderate-emission scenarios (SSP245 and SSP370), the Nei_3-4 relationship becomes significantly stronger, emerging as the dominant adjacency pattern, while Nei_1-2 weakens. This shift indicates that heat transfer pathways between functional zones play a more critical role as climate warming intensifies. In the high-emission scenario (SSP585), adjacency relationships become highly concentrated on Nei_3-4, with other adjacency connections weakening considerably. This pattern suggests that under extreme climate warming, deep connections between specific functional zones are essential for controlling energy consumption.

Across all future climate scenarios, adjacency relationships transition from a balanced and distributed model under TMY to a more specialized and concentrated configuration under SSP585. This trend implies that as climate change intensifies, buildings may require more precise control over inter-zone interactions to optimize energy efficiency. Regarding overall coordination and adaptation, the optimization results show a clear gradient shift from TMY to SSP585, indicating the need for gradual layout adjustments as climate change intensifies. A significant optimization strategy turning point in SSP245 suggests that moderate climate change may be a critical threshold for layout adaptation.

Conclusion

Under future climate scenarios, the evolution of energy efficient spatial layouts exhibits a nonlinear pattern, as reflected in the trends shown in Figures 9–11. While the orientation, division, and neighbor features remain broadly consistent across scenarios, the most notable transformations occur between SSP370 and SSP585. These inflection points highlight the nonlinear responsiveness of optimal building layouts to escalating climate pressures. Consequently, it becomes essential for architects to adopt phased and adaptive design strategies that accommodate both short-term fluctuations and long-

term shifts, thereby enhancing buildings' climate resilience across a spectrum of future conditions.

Design Recommendation

For short-term adaptation (TMY to SSP126), maintaining the advantage of the northeast-southwest orientation is recommended, along with a moderate increase in the proportion of the ZC_3 region and strengthened Nei_2-3 and Nei_3-4 connections. For mid-term adaptation (SSP245/SSP370), a significant increase in the proportion of east-west orientation should be implemented, accompanied by an expansion of the ZC_3 and ZC_4 regions and substantial reinforcement of the Nei_3-4 connection. For long-term adaptation (SSP585), east-west orientation should be established as the dominant strategy, with ZC_3 serving as the core zoning approach and a near-complete reliance on the Nei_3-4 adjacency relationship. For flexible design strategies, provisions should be made for potential orientation adjustments, reconfigurable zoning, and adaptable adjacency relationships to accommodate different climate scenarios.

As the climate scenario shifts from the TMY baseline to the SSP585 high-emission scenario, the optimal layout transitions from a diversified and balanced configuration to a specialized and concentrated strategy, underscoring the increasing need for precise spatial organization in response to intensifying climate change.

Outlook

This study explores the impact of different climate change scenarios on energy-efficient spatial layout in the context of climate change, summarizes the characteristics and variation patterns of energy-efficient spatial layout strategies under different climate scenarios, and provides comprehensive recommendations for achieving climate-adaptive building design. There are certain limitations in the current study. Including whether the three selected spatial layout features fully capture all characteristics, the effectiveness of interpretability methods for energy-efficient layouts, and the potential coincidence of results from a single building and city sample. Since this study uses operational energy consumption as the single evaluation metric, further research is needed to generalize the findings to urban samples in different regions or under varying socioeconomic contexts. Future work should take into account local climatic conditions, construction costs, land use constraints, and occupant comfort.

References

Andrić, I., Koc, M., & Al-Ghamdi, S. G. (2019). A review of climate change implications for built environment: Impacts, mitigation measures and associated challenges in developed and developing countries. *Journal of Cleaner Production*, 211, 83-102.

Du, T. (2021). *Space layout and energy performance: Parametric optimisation of space layout for the energy performance of office buildings* Delft University of Technology].

Du, T., Jansen, S., Turrin, M., & Van Den Dobbelsteen, A. (2020). Effects of architectural space layouts on energy performance: A review. *Sustainability*, 12(5), 1829.

Du, T., Jansen, S., Turrin, M., & van den Dobbelsteen, A. (2021). Effect of space layouts on the energy performance of office buildings in three climates. *Journal of Building Engineering*, 39, 102198.

Hemsath, T. L. (2013). Conceptual energy modeling for architecture, planning and design: Impact of using building performance simulation in early design stages.

IEA. (2019). *The critical role of buildings*. Retrieved from <https://www.iea.org/reports/the-critical-role-of-buildings>

Jähne, B. (2005). *Digital image processing*: Springer Science & Business Media.

Laflamme, E. M., Linder, E., & Pan, Y. (2016). Statistical downscaling of regional climate model output to achieve projections of precipitation extremes. *Weather and climate extremes*, 12, 15-23.

Latha, H., Patil, S., & Kini, P. G. (2023). Influence of architectural space layout and building perimeter on the energy performance of buildings: A systematic literature review. *International Journal of Energy and Environmental Engineering*, 14(3), 431-474.

Manni, M., Lobaccaro, G., Lolli, N., & Bohne, R. A. (2020). Parametric design to maximize solar irradiation and minimize the embodied ghg emissions for a zeb in nordic and mediterranean climate zones. *Energies*, 13(18), 4981.

Musau, F., & Steemers, K. (2008). Space planning and energy efficiency in office buildings: the role of spatial and temporal diversity. *Architectural Science Review*, 51(2), 133-145.

O'Neill, B. C., Kriegler, E., Riahi, K., Ebi, K. L., Hallegatte, S., Carter, T. R., . . . Van Vuuren, D. P. (2014). A new scenario framework for climate change research: the concept of shared socioeconomic pathways. *Climatic change*, 122, 387-400.

Riahi, K., Van Vuuren, D. P., Kriegler, E., Edmonds, J., O'Neill, B. C., Fujimori, S., . . . Fricko, O. (2017). The Shared Socioeconomic Pathways and their energy, land use, and greenhouse gas emissions implications: An overview. *Global environmental change*, 42, 153-168.

Shen, P. (2024). Building retrofit optimization considering future climate and decision-making under various mindsets. *Journal of Building Engineering*, 96, 110422.

Shen, P. (2025). Building and urban simulation under future climate: A novel statistical downscaling method for future hourly weather data generation. *Building Simulation*. doi:10.1007/s12273-025-1277-z

Shen, P., Ji, Y., Li, Y., Wang, M., Cui, X., & Tong, H. (2025). Combined impact of climate change and heat island on building energy use in three megacities in China. *Energy and Buildings*, 115386.

Shen, P., Li, Y., Gao, X., Chen, S., Cui, X., Zhang, Y., . . . Wang, M. (2025). Climate Adaptability of Building Passive Strategies to Changing Future Urban Climate: A Review. *Nexus*, 2(2), 1-13. doi:10.1016/j.nynexs.2025.100061

Shen, P., Li, Y., Gao, X., Zheng, Y., Huang, P., Lu, A., . . . Chen, S. (2025). Recent progress in building energy retrofit analysis under changing future climate: A review. *Applied Energy*, 383, 125441.

Tabadkani, A., Shoubi, M. V., Soflaei, F., & Banihashemi, S. (2019). Integrated parametric design of adaptive facades for user's visual comfort. *Automation in Construction*, 106, 102857.

Toutou, A., Fikry, M., & Mohamed, W. (2018). The parametric based optimization framework daylighting and energy performance in residential buildings in hot arid zone. *Alexandria engineering journal*, 57(4), 3595-3608.

Wang, H., & Zhai, Z. J. (2016). Advances in building simulation and computational techniques: A review between 1987 and 2014. *Energy and Buildings*, 128, 319-335.

Yukimoto, S., Kawai, H., Koshiro, T., Oshima, N., Yoshida, K., Urakawa, S., . . . Hosaka, M. (2019). The Meteorological Research Institute Earth System Model version 2.0, MRI-ESM2. 0: Description and basic evaluation of the physical component. *Journal of the Meteorological Society of Japan. Ser. II*, 97(5), 931-965.